EVALUATION OF A STALL-FLUTTER SPRING-DAMPER PUSHROD IN THE ROTATING CONTROL SYSTEM OF A CH-54B HELICOPTER

William E. Nettles
U.S. Army Air Mobility Research & Development Lab.,
Eustis Directorate, Ft. Eustis, Va.

William F. Paul and David O. Adams
Sikorsky Aircraft, Division of United Aircraft Corp.
Stratford, Conn.

Abstract

This paper presents results of a design and flight test program conducted to define the effect of rotating pushrod damping on stall-flutter induced control loads. The CH-54B helicopter was chosen as the test aircraft because it exhibited stall-induced control loads. Damping was introduced into the CH-54B control system by replacing the standard pushrod with spring-damper assemblies.

Design features of the spring-damper are described and the results of a dynamic analysis is shown which defined the pushrod stiffness and damping requirements. Flight test measurements taken at 47,000 lb gross weight with and without the damper are presented.

The results indicate that the spring-damper pushrods reduced high-frequency, stall-induced rotating control loads by almost 50%. Fixed system control loads were reduced by 40%. Handling qualities in stall were unchanged, as expected.

The program proved that stall-induced high-frequency control loads can be reduced significantly by providing a rotating system spring-damper. However, further studies and tests are needed to define the independent contribution of damping and stiffness to the overall reduction in control loads. Furthermore, the effects of the spring-damper should be evaluated over a range of higher speeds and with lower-twist blades.

Notation

AOB	angle of bank
CAS	calibrated airspeed, kt
C	damping rate, lb-sec/in.
C_M	blade section pitching moment coefficient
C/C_C	damping ratio
ERITS	equivalent retreating indicated tip speed, kt.
GW	aircraft gross weight
I	torsional moment of inertia
K	spring constant
K_D	damper spring rate, lb/in.
N_R	rotor speed
α	blade section angle of attack
θ_{75}	blade angle at 75% rotor radius
ω	torsional natural frequency, cycles/sec
ω/Ω	ratio of natural frequency to rotor frequency

Presented at the AHS/NASA-Ames Specialists' Meeting on Rotorcraft Dynamics, February 13-15, 1974.

Introduction

Control system loads can limit the forward speed and maneuvering capability of high performance helicopters. The slope of the control load buildup is often so steep (Figure 1) that it represents a fundamental aeroelastic limit of the rotor system. This limit cannot be removed by strengthening the entire control system without incurring unacceptable weight penalties.

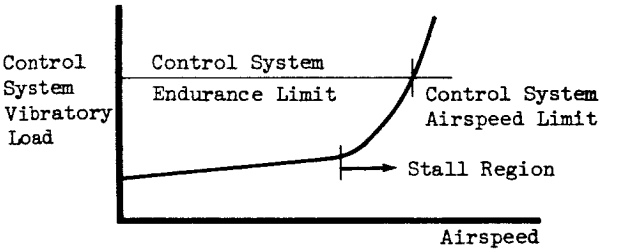

Figure 1. Control Load Characteristic

Studies of the problem reported in Reference 1-7 indicate that the abrupt increase in control loads is induced by high-frequency stall-induced dynamic loading. This loading is attributable to a stall-flutter phenomenon which occurs primarily on the retreating side of the rotor disc in high advance ratio and/or high load factor flight regimes. At the relatively high retreating blade angles of attack which occur under these conditions, the blade section experiences unsteady aerodynamic

stall and the moment coefficient varies with the time-varying angle of attack as shown in Figure 2. Inspection of the moment hysteresis loops exhibited in this figure indicate that positive work can be done on the system as the blade section oscillates in torsion. This aeroelastic mechanism, by which energy is added to the system, can be termed "negative damping" and produces pitch oscillations of increasing amplitude at the blade/control system natural frequency. The rotor system is therefore more responsive to rotor loading harmonics which are close to the blade torsional frequency, and the end result is a rapid buildup of higher harmonic control loads during maneuvers and high-speed flight.

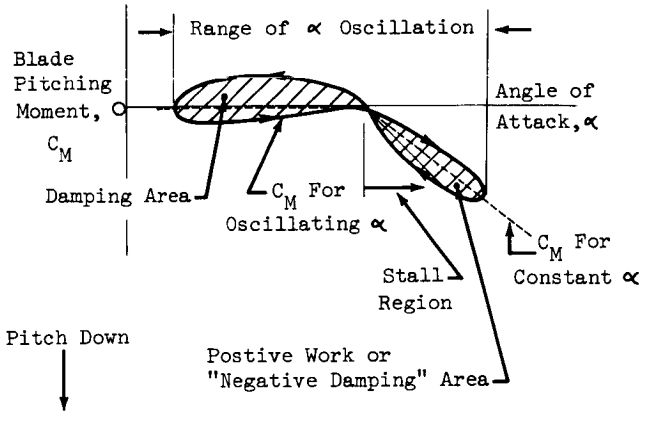

Figure 2. Pitching Moment Hysteresis Loops.

The response of the rotor system is usually stable, because the blades are moving into and out of the negative damping region once per revolution. However, during maneuvers in which a significant portion of the rotor disc is deeply stalled, very large oscillations can exist (Reference 7) and the negative damping region can increase to a point where blade oscillations can continue into the advancing portion of the rotor disc.

Efforts to understand the problem have centered on defining unsteady aerodynamic characteristics of the blades in stall (References 4 and 6) and on incorporating this data into blade aeroelastic computer analyses (References 6 and 9). Results of the studies are encouraging. The buildup of control loads and high-frequency stall-induced loads is predicted with reasonable accuracy.

Recognizing that the basic cause of the problem was insufficient pitch damping, the Eustis Directorate contracted with Sikorsky Aircraft to evaluate the effects of pushrod spring-dampers on control loads of the CH-54B helicopter. This helicopter was selected for the study since it exhibited high-frequency stall-induced control loads during maneuvers at maximum speeds and 48,000 pounds gross weight and was available to the program. Rotating pushrod dampers were used instead of fixed system dampers because they provided the required damping directly at the blade attachment. The program was limited in scope to an analytical and experimental feasibility study of the concept, and was conducted in four phases.

(1) Dynamic Analysis

(2) Functional Design

(3) Ground Tests

(4) Flight Test Evaluation

Dynamic Analysis

An aeroelastic analysis of the CH-54B rotor was performed to evaluate the effectiveness of spring-dampers in reducing the control loads associated with retreating blade stall-flutter and to evolve design criteria. The primary mathematical analysis used was the Normal Modes Rotor Aeroelastic Analysis Y200 Computer Program. This analysis, which is described in Reference 8, represents blade flatwise, edgewise, and torsional elastic deformation by a summation of normal mode responses and performs a time-wise integration of the modal equations of motion. This analysis can also be used to study blade transient response following a control input or disturbance. Aerodynamic blade loading is determined from airfoil data tabulated as a function of blade section angle of attack, Mach number, and first and second time derivatives of angle of attack. Unsteady aerodynamics and a nondistorted helical wake inflow were used throughout this investigation.

The version of the Y200 Program used for this study is a single-blade, fixed-hub analysis. The assumptions were made that all blades are identical and encounter the same loads at given azimuthal and radial positions and that blade forces and moments do not cause hub motion. Any phenomena which are related to nonuniformity between blades or to the effect of hub motion on blade response are not described by this analysis.

Free Vibration Characteristics

For a blade restrained at the root by a pushrod, the first step in the aeroelastic analysis is the calculation of the undamped natural frequencies and modes for a blade rotating in a vacuum. In order to analyze the spring-damper/blade system using the normal modes procedure, the damped free vibration modes and frequencies were calculated based on the model shown in Figure 3. The torsional system was represented by fifteen elastically-connected lumped inertias restrained in torsion by a spring-damper at the blade root. The eigenvalues and eigenvectors of the system response were calculated using a Lagrangian formulation of the damped free vibration equations. A radial mode

shape, natural frequency and modal damping were calculated and used in the Y200 Program.

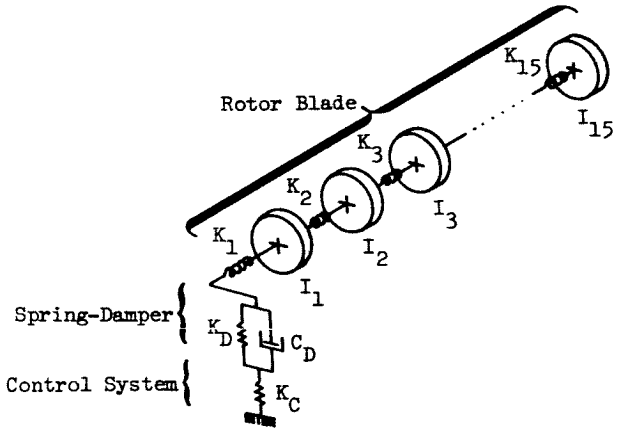

Figure 3. Schematic of the Spring-Damper Free Vibration Problem.

Spring-Damper Behavior

The behavior of the CH-54B spring-damper was determined by employing the free vibration analysis to determine the general relationship between the properties of the damper itself and those of the blade first torsional mode. Figure 4 shows the variation of blade first torsional natural frequency and percent critical damping with changes in the spring and damping constants of the spring-damper.

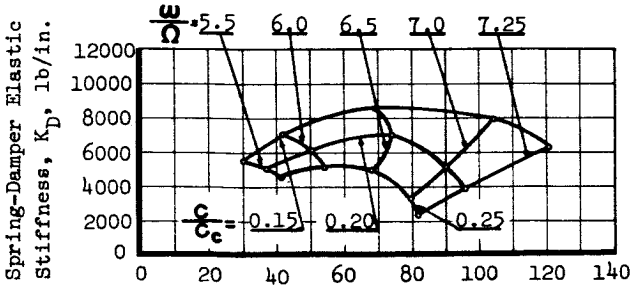

Figure 4. Effect of Spring-Damper Properties on First Torsional Mode Frequency and Damping.

Three trends are evident from this figure:

1. For a given damper spring constant, K_D, high levels of damping can increase the root dynamic stiffness enough to result in torsional natural frequencies which are close to those obtained with a rigid pushrod. It is clear from Figure 4 that as the damping constant, C_D, is increased, the damper spring is effectively bridged so that the torsional natural frequency approaches the standard pushrod value (7.4 per rev.)

2. For each spring constant, K_D, a specified value of the damping constant, C_D, maximizes the modal damping. Increasing or decreasing the damping constant decreased the percent critical damping ratio of the torsional vibration.

3. The variation in the percent critical damping parameter with damping constant is relatively gradual, so small manufacturing differences between the six production dampers will not cause great differences in first torsional mode damping.

Rotor System Analysis

For the initial analytical comparison of the control system loading with and without damping, prior to design of actual hardware, a representative flight condition was selected for which experimental data existed for the conventional system. This data was extracted from the structural substantiation flight tests of the CH-54B and represents a condition in which stall-induced dynamic loading was experienced. The specific flight condition used - gross weight 47,000 lb, 100% Rotor Speed (185 RPM), sea level standard, 30° angle of bank right turn- was selected because it was the condition which consistently produced stall-induced high-frequency loading. The plot of rotating pushrod load against azimuth for this condition is shown in Figure 5a.

The pushrod load resulting from the Y200 Normal Modes Program for the same flight condition is compared with flight test results in Figure 5b. To account for the increase in rotor lift experienced in the turn, a lift of about 60,000 lb and a propulsive force of 3,300 lb was calculated. Although the calculated pushrod load shows a significantly greater steady nose-down load, the vibratory amplitude and frequency content of the analytical result match the test reasonably well.

To study the effectiveness of the spring-damper in reducing vibratory control loads, the flight condition described above was simulated using several spring-damper configurations. Each of these cases was run with the same control settings as the standard case. The results are shown in Figure 6. As shown, the combination of 5000 lb/in. and damping between 50 and 90 lb-sec/in. was about optimum. Referring back to Figure 4, it is seen that a damping value of 90 lb-sec/in. would provide a frequency of 7P which was the same as the standard aircraft. This configuration was therefore selected because the test results could then be used to evaluate the spring-damper at the same torsional frequency as the

standard aircraft. Also it would provide an option to reduce the damping in follow-on programs to allow an evaluation at 5.5/rev and 20% critical damping.

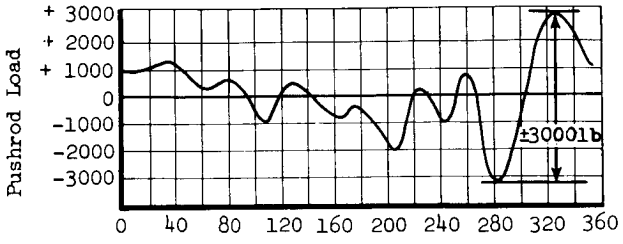

Figure 5a. Measured Flight Test Result.

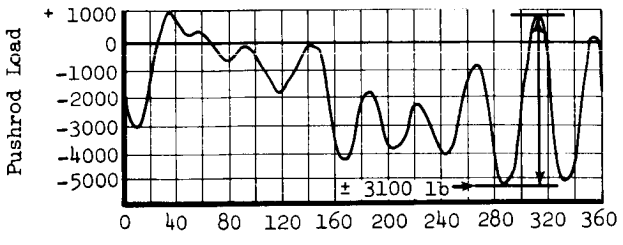

Figure 5b. Derived Result.

Figure 5. Comparison of Measured and Derived Conventional Pushrod Load - CH54B, 47000 lb G.W., Sea Level, 100 KT, 30° AOB Right Turn.

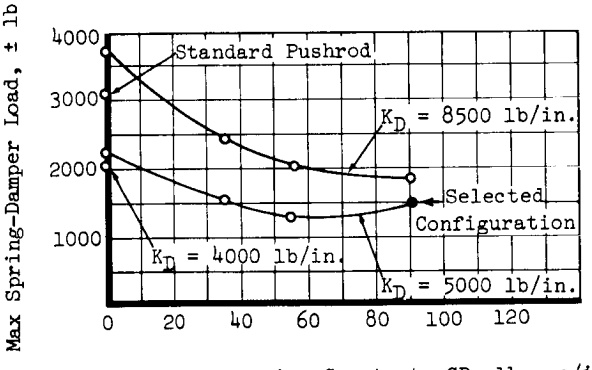

Figure 6. Effect of Spring-Damper Parameters on the Amplitude of Vibratory Control Loads

The plots of pushrod load against azimuth shown in Figure 7 compare a standard pushrod with a spring-damper having a spring rate of 5,000 lb/in. and a damping rate of 90 lb-sec/in. For this configuration the free vibration analysis gives a torsional frequency of 7 per rev and 0.20 critical damping ratio. The Figure shows approximately equal amounts of one-per-rev variation occurring in the control load time-histories since the pushrod spring-dampers do not affect the low-frequency torsional motion. As a result, the overall peak-to-peak control load is reduced by only 25%, while the high-frequency retreating blade control loads are reduced by more than 50%. It is these high-frequency loads that cause the 6 per rev control system loads in the fixed system.

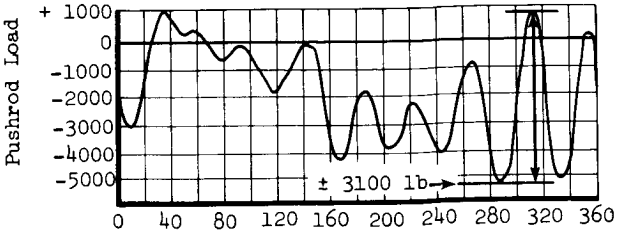

Figure 7a. Conventional Pushrod.

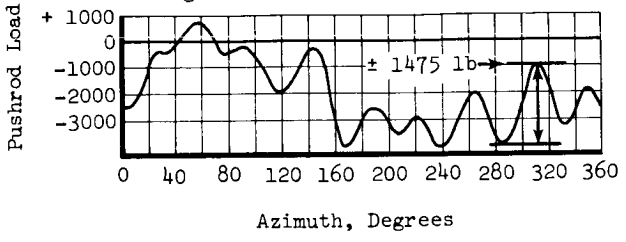

Figure 7b. Stall-Flutter Spring-Damper, K_D = 5000 lb/in., C_D = 90 lb-sec/in.

Figure 7. Comparison of Derived Conventional Pushrod Load and Spring-Damper Load - CH-54B, 47000 lb G.W., Sea Level, 100 KT, 30° AOB Right Turn.

It is clear from this analysis that (1) damping at the blade root is effective in reducing control loads for a given root stiffness and (2) reducing root stiffness tends to decrease the loads for a given damping constant (at least for the ranges investigated).

Functional Design

Design Requirements

The aeroelastic analysis indicated that spring and damping introduced at the blade root could significantly reduce stall-induced loads. The most favorable location for the test of a blade root spring-damper is at the pushrod connecting the rotating swashplate to the blade horn, since the existing pushrod may be replaced easily with the spring-damper. It was determined that a spring-damper device could be fabricated to replace the conventional pushrod, provided that the restrictive size limitations could be met. The use of an elastomer as the primary structural member met the size and spring rate requirements.

The design requirements, based on the aeroelastic analysis and the planned test programs, are summarized as follows:

- Replace Conventional Pushrod
- Life - 50 hr

- Load - ±5,000 lb
- Spring Rate - 5,000 lb/in.
- Damping Rate - 90 lb-sec/in.
- Maximum Elastic Deflection - ±1/2 in.
- Adjustable for Blade Tracking
- Fail-Safe Design

Principles of Operation

The final configuration of the stall-flutter spring-damper pushrod designed to meet the above requirements is shown in Figures 8 and 9.

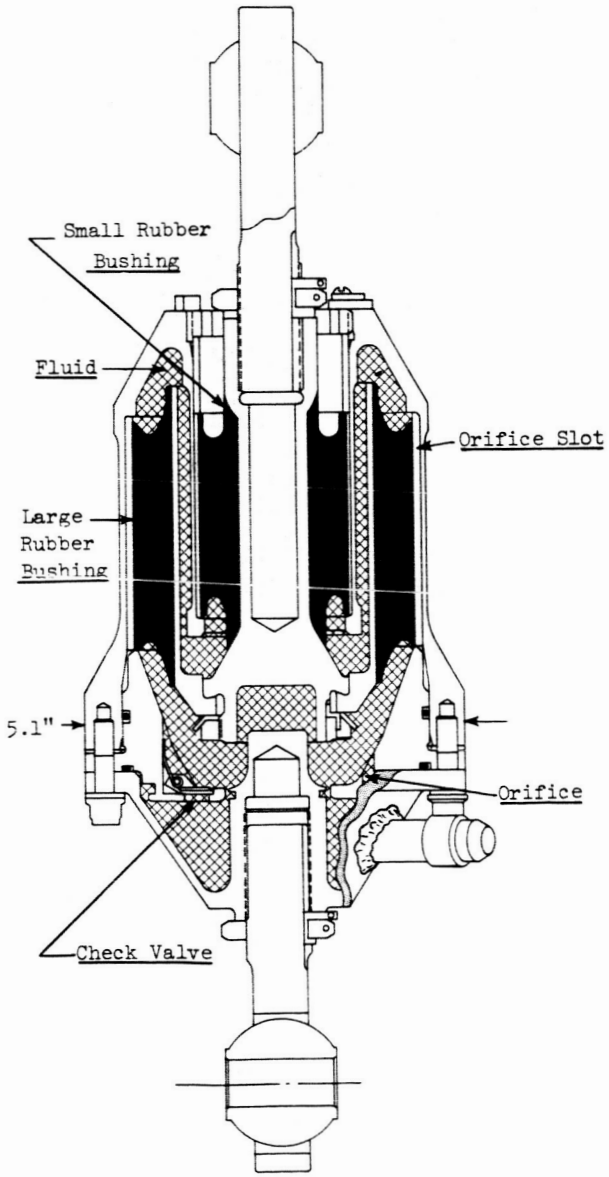

Figure 8. Stall-Flutter Spring-Damper Pushrod Assembly.

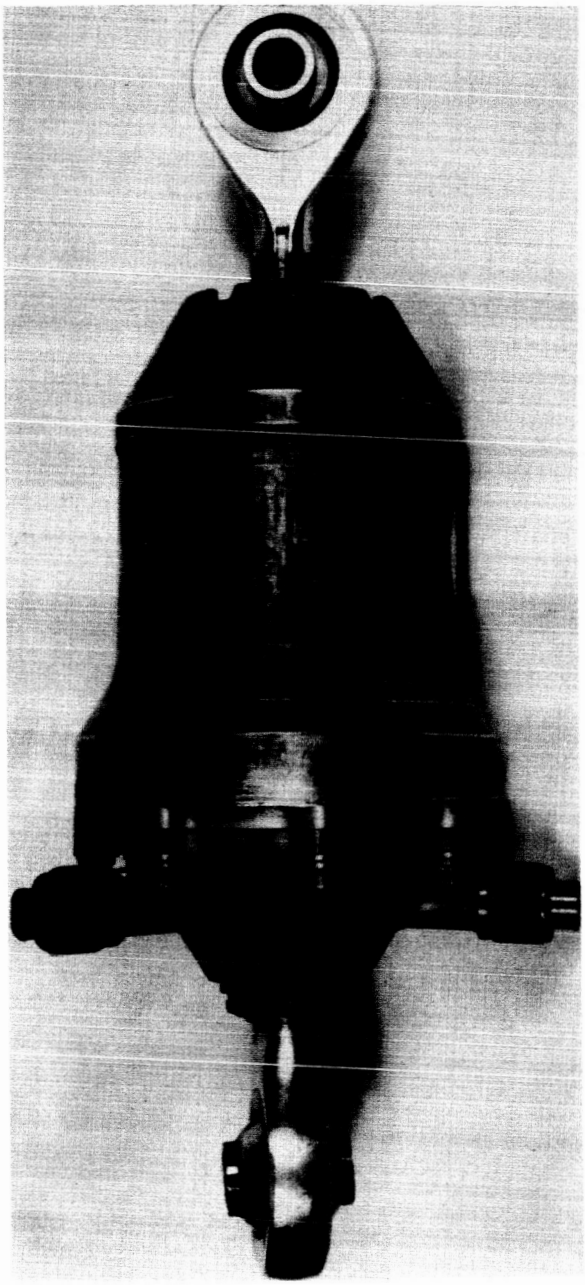

Figure 9. Stall-Flutter Spring-Damper Pushrod.

The concept consists basically of a piston restrained in a cylinder by two natural rubber elastomeric bushings which provide the required spring rate. Damping is obtained by displacement of fluid through orifices. The bushings are mounted in parallel, thereby providing a fail-safe design. In addition, physical stops are incorporated to limit spring-damper deflection to ± 1/2 inch in the event of overload or complete rubber failure. No sliding action takes place as the spring-damper is deflected. Elastomeric elements were chosen because of their high allowable

strains, integral hydraulic sealing, and compactness. An integral air-oil accumulator was found to be inadequate and an external accumulator system was used in the ground and flight tests.

Ground Tests

A comprehensive ground test program was conducted to develop the required performance of the spring-damper, to demonstrate structural adequacy and safety for the flight tests, and to evaluate the performance of an installed spring-damper system. This was accomplished by the means of single unit dynamic performance and fatigue tests, flight unit proof and operation tests, and an installed system whirl tests utilizing the flight test spring-dampers and rotor blades.

Flight Test Evaluation

The performance of the stall-flutter spring-damper pushrod system installed on a CH-54B helicopter was evaluated in a series of flight tests consisting of: (1) base-line flights of the CH-54B helicopter in standard configuration, and (2) comparison flights with the spring-damper system installed.

The investigation was limited to the feasibility of the damper and did not extend to an extensive evaluation of the overall effect on the CH-54B operating envelope.

Baseline Flights

A short series of baseline flights was conducted on the instrumented test aircraft in standard configuration in order to obtain up-to-date performance and control load data.

Of the several conditions flown, the 115 kt, 96% rotor speed, level flight point was the best stall condition from the standpoint of uniformity and repeatability. The maximum pushrod vibratory load observed was about ± 2,100 lb. This is lower than some stall results observed in the past on this aircraft, but the typical stall-flutter characteristic was observed in the pushrod time histories and was therefore adequate for baseline purposes.

Spring-Damper Pushrod Tests

The spring-damper pushrods were installed on the CH-54B rotor head as shown in Figure 10 and 11. Flight test time histories of rotating pushrod load for rigid pushrods and for the spring-damper pushrods at 47,000 lb gross weight are shown in Figures 12 and 13. These segments of data which depict the time history for approximately 1-1/2 revolutions were selected as representative samples from oscillograph traces in which the waveform was continuously repeated for more than 15 revolutions.

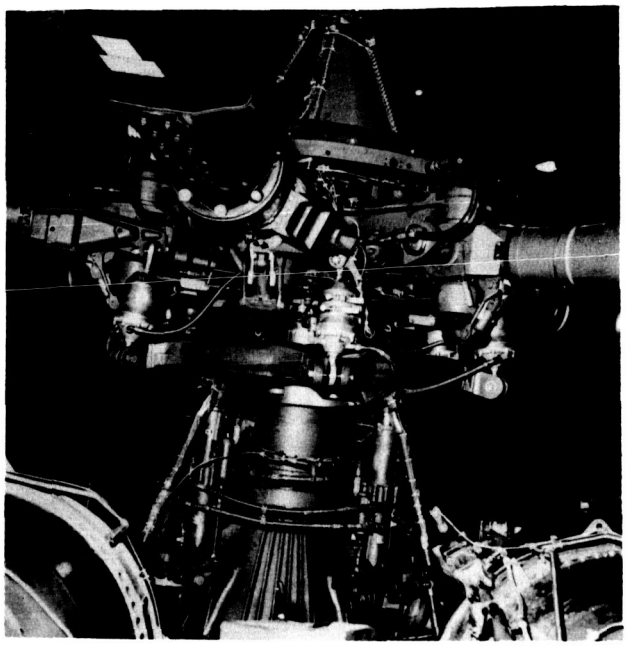

Figure 10. Spring-Damper System Flight Aircraft Installation.

Figure 11. First Flight of the Spring-Damper System, February 6, 1973.

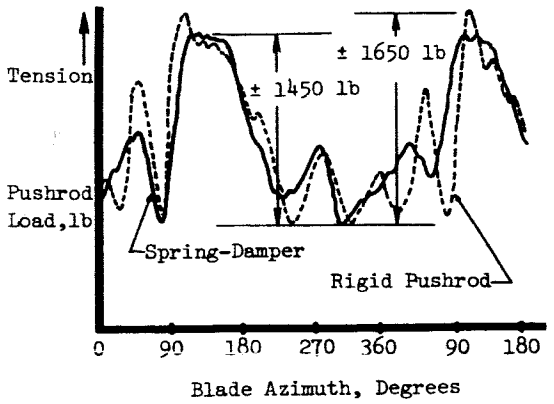

Figure 12. Rotating Pushrod Load Comparison 110 KT 96% N_R Level Flight, 4700 lb.

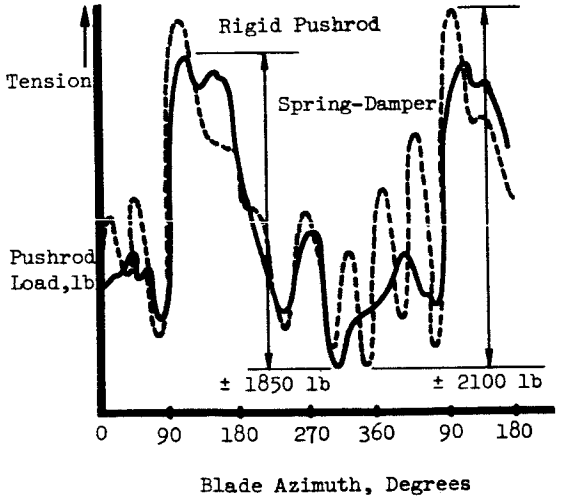

Figure 13. Rotating Pushrod Load Comparison 115 KT 96% N_R Level Flight, 47000 lb GW.

As shown, the rigid pushrod record exhibits the high-frequency oscillation beginning on the retreating side which is characteristic of the stall-flutter phenomenon. This frequency was between 7 and 8 per rev and compares well with the calculated system torsional natural frequency of 7.4 per rev. As seen, the high-frequency loads were significantly reduced with the spring-damper pushrods. The overall reduction was smaller because the low-frequency response was not reduced. This was expected because the high twist blades produce large 1p loads and the spring-damper was not designed to reduce these loads. As shown, the results demonstrate a reduction of almost 50% in high-frequency loads. A spectral analysis of the data burst which contains this cycle is shown in Figure 14.

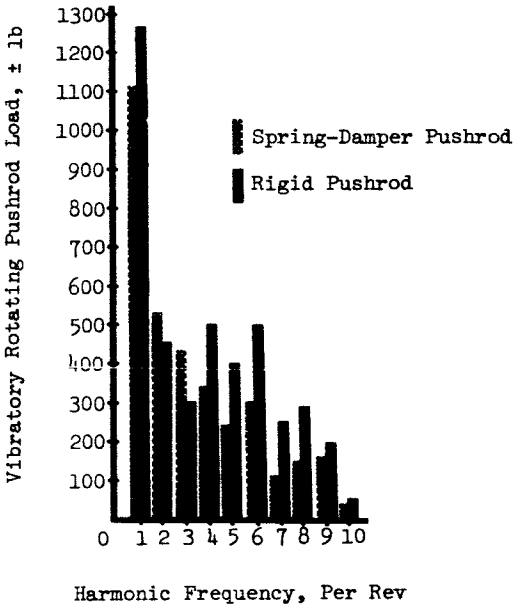

Figure 14. Comparison of Spectral Analyses - CH-54B, 47000 lb G.W., 115 KT 96% N_R Level Flight, 2000' Altitude.

Comparison of Stationary Control Loads

Flight test time-histories of right lateral stationary star load for rigid pushrods and for spring-damper pushrods are shown in Figure 15. These records show the expected dominance of the 6 per rev response in a 6-bladed rotor. As shown, stationary control loads were reduced by 40% for the spring-damper case.

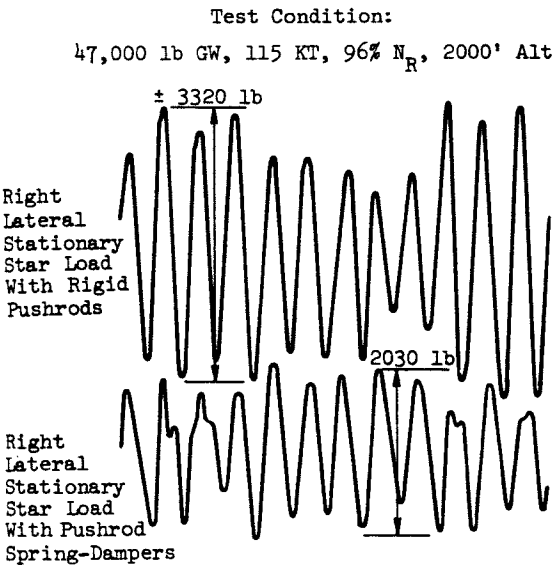

Figure 15. Comparison of Stationary Control Loads.

A plot of stationary control load against ERITS (Equivalent Retreating Indicated Tip Speed) is shown and defined in Figure 16. The sharp increase in load as stall is entered is seen to be unchanged by the damper installation, but as the aircraft goes deeper into the stall region, the loads are reduced.

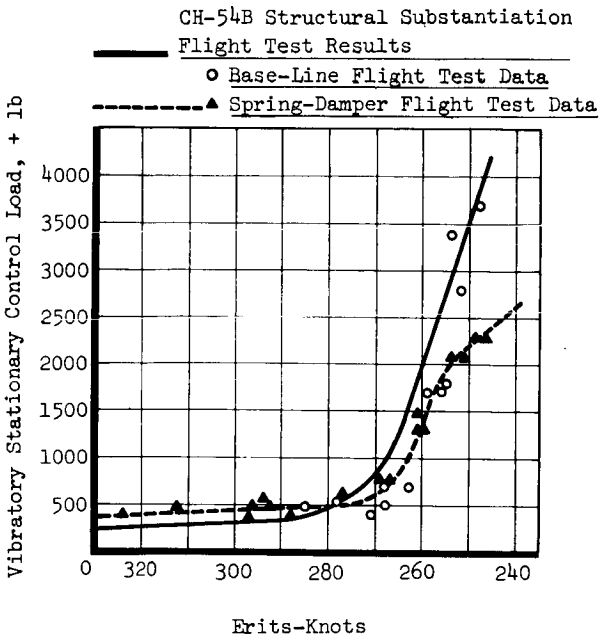

Figure 16. Stationary Control Load Against Erits

Note: Erits - Equivilent Retreating Indicated Tip Speed

$$= \frac{\text{Rotating Tip Speed} \times \sqrt{\text{Air Density Ratio}} - \text{CAS}}{\sqrt{\frac{\text{Load Factor} \times \text{Gross Weight}}{37{,}500}}}$$

Comparison of Aircraft Handling Qualities

The handling qualities of the aircraft were unchanged with the spring-dampers installed. Pilot's reports state that the aircraft exhibited the characteristic increase in vibration, difficulty in maintaining airspeed, and forward control motion required when approaching a stall condition in both the baseline and spring-damper flights. The stalled condition of the rotor appears unaffected by the installation of the spring-damper. Blade stresses and blade motions (except for the stall-flutter torsional oscillation) are virtually the same in each case. Cockpit vibration levels are unchanged. This was expected because the stall was not changed, just the local torsional response of the blade was changed.

The effect of the damper on the control system can be seen in plots of control positions against airspeed (Figure 17). The lateral control is unaffected, but as much as 10% more forward longitudinal control is required when flying at the 115 kt, 96% N_R reference stall condition.

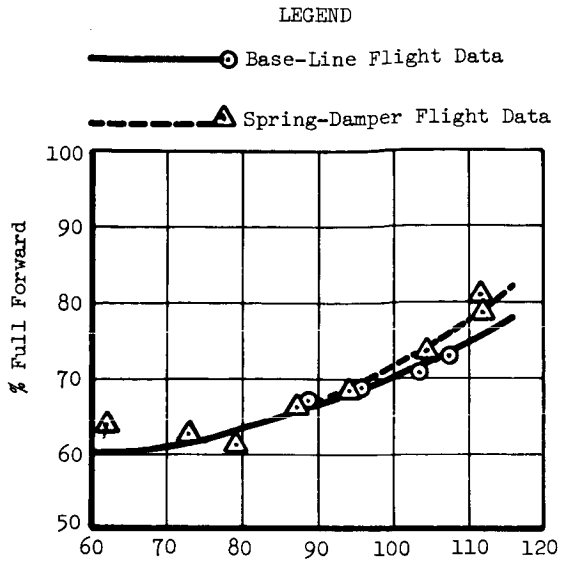

Figure 17a. 100% Rotor Speed.

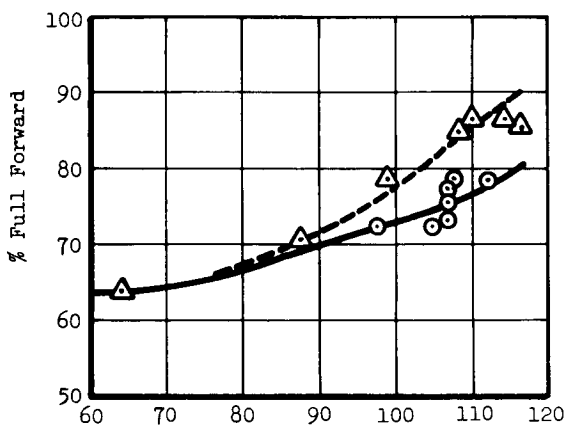

Figure 17b. 96% Rotor Speed

Figure 17. Longitudinal Control Positions.

Aeroelastic Analysis of Flight Test Data

Following completion of flight testing, three additional computer analysis conditions were run, using test conditions actually observed in the flight tests. The methods used were the same as described earlier with the exception that a calculated lift higher than the gross weight actually flown was used. The amplitudes of pushrod load predicted were much lower than observed using the correct lift, and since the comparison with and without the spring dampers was of primary interest, the calculated lift was increased. This shows that improvement in the

analysis is needed.

Figure 18 shows pushrod load vs azimuth for the 115 kt, 96% N_R reference condition for conventional pushrods as generated by the aeroelastic analysis and as observed in the baseline flight. The analysis again shows a good correlation in wave shape with test result. Based on analysis of force-displacement phase shifts seen in the flight test results, a damping rate of 70 lb-sec/in. was determined to be a likely value actually achieved. Figure 18 also compares the analytical result with the flight test result.

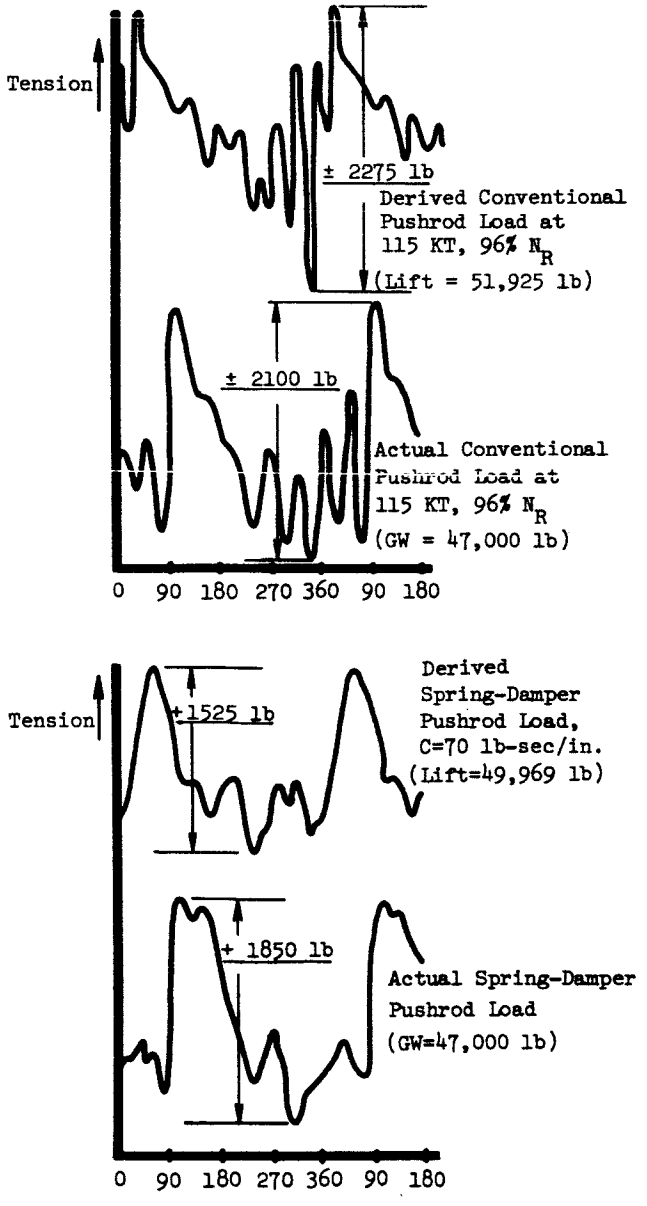

Figure 18. Comparison of Measured and Derived Pushrod and Spring-Damper Loads.

A good correlation in wave shape is obtained. However, the sharp reduction in peak-to-peak amplitude over the rigid pushrod case as predicted by the aeroelastic analysis is again not achieved in practice. It should be noted that the aeroelastic analysis assumes that all blades and spring-dampers are identical, which is known not to be case. Difference among spring-dampers would at least contribute to the dominant one-per-rev component and perhaps the harmonics as well.

Conclusions

It is concluded that:

1. Stall-flutter spring-damper pushrods located in the rotating control system effectively reduced stall-induced high-frequency rotating control loads on the CH-54B by almost 50% and overall stationary control loads by more than 40%.

2. The spring-damper pushrod system does not significantly alter the performance or handling qualities of the CH-54B helicopter.

Recommendations

The test results were very encouraging, but as usual raised more questions than it answered. Some of these are stated below:

1. The combination of a spring and damping worked well, but quantatively what was the contribution of each?

2. Would lower twist, higher mach number and lower frequency provide different results?

3. Would a high-speed aircraft show some improvement in performance in stall with the spring-damper?

To help answer these questions, the CH-54B rotor system could be installed on an H53 helicopter and flown to high speed. Damping, torsional frequency, and twist could easily be varied to qualify their effects. Plans to accomplish this are underway.

References

1. Harris, F. D., and Pruyn, R. R., BLADE STALL - HALF FACT, HALF FICTION, American Helicopter Society, 23rd Annual National Forum Proceedings, AHS Preprint No. 101, May, 1967.

2. Ham, N. D., and Garelick, M. S., DYNAMIC STALL CONSIDERATIONS IN HELICOPTER ROTORS, Journal of the American Helicopter Society, Vol. 13, No. 2, April 1968, pp. 49-55.

3. Ham, N. D., AERODYNAMIC LOADING ON A TWO-DIMENSIONAL AIRFOIL DURING DYNAMIC STALL, AIAA Journal, Vol. 6, No. 10, October 1968, pp 1927-1934.

4. Liiva, J., et al., TWO-DIMENSIONAL TESTS OF AIRFOILS OSCILLATING NEAR STALL, Vol. I, Summary and Evaluation of Results, The Boeing Company, Vertol Division; USAAVLABS TR 68-13A, U. S. Army Aviation Materiel Laboratories, Fort Eustis, Virginia, April 1968, AD 670957.

5. Carta, F. O., et al., ANALYTICAL STUDY OF HELICOPTER ROTOR STALL FLUTTER, American Helicopter Society, 26th Annual National Forum, AHS Preprint No. 413, June, 1970.

6. Arcidiacono, P. J., et al., INVESTIGATION OF HELICOPTER CONTROL LOADS INDUCED BY STALL FLUTTER, United Aircraft Corporation, Sikorsky Aircraft Division; USAAVLABS Technical Report 70-2, U. S. Army Aviation Materiel Laboratories, Fort Eustis, Virginia, March 1970, AD 869823.

7. Carta, F. O., and Niebanck, C. F., PREDICTION OF ROTOR INSTABILITY AT HIGH FORWARD SPEEDS, Vol. III, Stall Flutter, United Aircraft Corporation, Sikorsky Aircraft Division; USAAVLABS Technical Report 68-18C, U. S. Army Aviation Materiel Laboratories, Fort Eustis, Virginia, February 1969, AD 687322.

8. Arcidiacono, P. J., STEADY FLIGHT DIFFERENTIAL EQUATIONS OF MOTION FOR A FLEXIBLE HELICOPTER BLADE WITH CHORDWISE MASS UNBALANCE, USAAVLABS TR-68-18A, February 1969, AD 685860.

9. Carta, F. O., et al., INVESTIGATION OF AIRFOIL DYNAMIC STALL AND ITS INFLUENCE ON HELICOPTER CONTROL LOADS, USAAVLABS TR72-51, Eustis Directorate, U. S. Army Air Mobility Research and Development Laboratory, Fort Eustis, Virginia, September 1972, AD 752917.